AIP | Journal of Applied Physics

Alternated high- and low-pressure nitriding of austenitic stainless steel: Mechanisms and results

G. F. Gomes, M. Ueda, and H. Reuther

Citation: J. Appl. Phys. **94**, 5379 (2003); doi: 10.1063/1.1614429
View online: http://dx.doi.org/10.1063/1.1614429
View Table of Contents: http://jap.aip.org/resource/1/JAPIAU/v94/i8
Published by the American Institute of Physics.

Additional information on J. Appl. Phys.

Journal Homepage: http://jap.aip.org/
Journal Information: http://jap.aip.org/about/about_the_journal
Top downloads: http://jap.aip.org/features/most_downloaded
Information for Authors: http://jap.aip.org/authors

ADVERTISEMENT

Downloaded 13 May 2013 to 150.163.34.35. This article is copyrighted as indicated in the abstract. Reuse of AIP content is subject to the terms at: http://jap.aip.org/about/rights_and_permissions

Alternated high- and low-pressure nitriding of austenitic stainless steel: Mechanisms and results

G. F. Gomes[a] and M. Ueda
National Institute for Space Research, Associated Laboratory of Plasma-LAP/INPE, Av. dos Astronautas, 1758, CEP 12221-010, São José dos Campos-SP, Brazil

H. Reuther
Institute of Ion Beam Physics and Materials Research, Forschungszentrum Rossendorf, FZR, Dresden, Germany

(Received 10 March 2003; accepted 6 August 2003)

A combined surface modification treatment consisting of ion nitriding at high pressure and high temperature, followed by a cycle at low pressure, both cycles using a gas mixture of (N_2/H_2):(50/50) in pressure, was applied to stainless-steel AISI 304. In the first cycle, in a glow discharge at 4×10^{-1} mbar and temperatures of 400–450 °C, high-pressure nitriding was applied to the samples. In the second cycle, in a glow discharge at 8×10^{-4} mbar, low-pressure nitriding was applied to the samples. Applying this sequential hybrid treatment alternately, good nitriding was obtained. X-ray diffraction (XRD) measurements showed the effects of this hybrid ion nitriding in the AISI 304 surface, indicating thick nitrided layers, confirmed by Auger electron spectroscopy (AES). Conversion electron Mössbauer spectroscopy, combined with AES and XRD, showed phases and compounds induced by such treatments. Vickers hardness measurements showed great enhancement in the surface hardness. Applying other combinations of gas mixtures and cycles, produced diverse results in the surface, like the induction of α- and ϵ-phases. © *2003 American Institute of Physics.* [DOI: 10.1063/1.1614429]

I. INTRODUCTION

Ion nitriding or plasma nitriding of metal parts, in particular those made of steel and cast iron, is extensively applied in the manufacturing industries nowadays.[1,2] It is a proven technology which is used to improve the surface properties, providing fatigue life, wear, and corrosion resistance enhanced components. Normally, in ion nitriding of steels, temperatures from 400 °C to 650 °C are required to produce useful modified surfaces. The component being treated is biased as a cathode of a pure N_2 or a mixture of N_2/H_2 glow discharge, running in dc (typically 400 to 1000 V) or pulsed modes (frequencies of up to tens of kHz). The nitrogen ions present in the plasma discharge are adsorbed on the surface of the component, and through a complex physico-chemical process therein being thermally diffused into deep layers, ranging from few to tens of μm. However, to obtain useful modified layers, nitriding times as long as tens of hours are necessary.[3] The advent of techniques, like plasma immersion ion implantation and hybrid treatments, led to optimized processes.[4–8]

The uptake of nitrogen into the surface layer can produce several modifications. As the nitrogen atomic concentration grows in the region and solid interstitial solution of N exceeds the solubility limit, precipitation of the steel components nitrides would occur. For instance, in AISI 304, which have a composition of 18% Cr, 8%–10% Ni, and Fe to balance, nitriding can produce MN, M_2N, and so on, where M=Cr, Fe, and possibly Ni, and N=nitrogen, forming the compound layer.[9] A more selective formation of some nitrides depends on the process parameters, like gas composition, nitrogen ion density, pressure, sample temperature, and bias voltage.[6] Among the most desirable nitrides to be synthesized in the compound layer, are the Fe_4N, also called γ' and the $Fe_{2-3}N$, the ϵ phase.[10,11] These nitrides have good tribological properties, like enhanced hardness, reduced wear rate, and friction and in some cases, an improvement in the corrosion resistance. The nitrogen ions, driven by thermally activated diffusion, can penetrate far beyond the compound layer. These nitrogen atoms, uptaken into the austenitic stainless-steel lattice, produce a solid solution, the γ_N phase, also called expanded austenite, as a slight expansion in the lattice parameter occurs. Owing to this expansion, there is a considerable increase in the surface hardness.[12–16]

Another approach to ion nitriding involved samples of austenitic stainless-steel AISI 304 which were treated alternating two cycles at different conditions.[17] The first cycle consists of a high-pressure nitriding (HPN), at 4×10^{-1} mbar, when the samples reach temperatures of about 450 °C. The second cycle consists of a high temperature, that is attained in the first cycle, low-pressure nitriding (LPN) at 8×10^{-4} mbar. Thus, the whole process takes advantage of the high temperature attained in the first cycle, which prepares the samples for the second cycle, when in the low-pressure plasma, the higher mean-free path of the accelerated nitrogen ions allows a greater final kinetic energy, compared to that of the ions available in the first cycle. This type of nitriding offers no problems with arcing, as the first cycle can be run at low bias voltages, enough only to heat the samples. In the second cycle, operating the system at low

[a]Electronic mail: gfgomes@plasma.inpe.br

 © 2003 American Institute of Physics

Downloaded 13 May 2013 to 150.163.34.35. This article is copyrighted as indicated in the abstract. Reuse of AIP content is subject to the terms at: http://jap.aip.org/about/rights_and_permissions

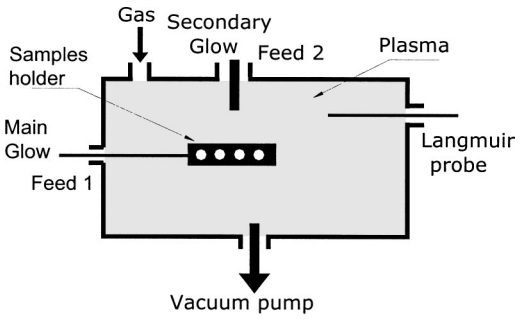

FIG. 1. Schematics of the vacuum vessel and ancillaries used to the nitriding experiments at Laboratório Associado de Plasma, LAP-INPE/Brazil.

pressure, with the plasma being generated by an independent source, there is no arcing between the samples and the chamber ancillaries, even at much higher bias voltages. Good uniformity of the treated surface is obtained, as the more diffuse plasma produces less or no points of high ion concentration, where, if so, a high current density could induce a higher local temperature, with possible surface damages. Other advantages of this approach are:

(1) There is no need for an auxiliary heating system, as is used in conventional nitriding which requires cumbersome heaters consuming large electrical powers,
(2) Small system, 30 liter chamber,
(3) Simple and low cost electrical power system for plasma production and biasing of the samples.

II. EXPERIMENTAL PROCEDURE

The experimental setup used for this sequential treatment is shown in Fig. 1. The 30 liter vacuum chamber and the low-pressure plasma source based on glow discharge are the ones used in the previous experiments with plasma immersion ion implantation.[18] For the present experiments, two feedthroughs are used to power the glow discharges. The main dc power supply used for the high-pressure glow discharge nitriding is applied to feed 1. The high-voltage bias to the low-pressure nitriding is also applied through this feed. A secondary dc voltage supply is used for the low-pressure glow discharge, which is fed into the chamber through feed 2. This glow discharge runs at 900 V and 80 mA, at 8×10^{-4} mbar, with N_2 or (N_2/H_2) gas mixture.

The samples of AISI 304 were disks of 15 mm diameter and 3 mm thickness, polished to 1 μm with alumina powder. Prior to treatment, all samples were cleaned in an acetone ultrasonic bath. After entering the chamber, before the application of nitriding process, sputter cleaning was applied. The treatment under discussion consists of applying two nitriding cycles. The first one consisted of HPN and feeding gas mixture of (N_2/H_2):(50/50) in pressure, called a standard gas mixture. The discharge was run at -600 to -800 V and currents of 250 mA. In this cycle, the samples reached 400–450 °C. We run this mode for 15 min. The second cycle, LPN, consisted of applying a bias voltage of -700 V to the samples immersed in glow discharge plasma of the standard gas mixture. The current reached 30–40 mA. In this cycle, we take advantage of the high temperature attained in the first cycle, as this current alone is not enough to heat the samples. This cycle was run for 15 min, also. At the end of this cycle, the temperature of the samples was about 300 °C. We performed five of each cycle alternately, performing a total of 150 min of nitriding. As a matter of comparison, we tested other gas compositions and nitriding sequences, as there are some questions about the efficacy of the nitrogen/hydrogen mixture[19–21] and, so far, a complete understanding of the composition effect on the nitriding mechanisms is still missing.[22]

For the measurement of the sample temperature along the treatment, we used a RayTek infrared pyrometer. For the measurements of x-ray diffraction of nitrided 304 stainless-steel samples, a Philips 3410 diffractometer in the standard 2θ mode and Ni-filtered Cu $K\alpha$ radiation was used. Hardness tests were carried out in a Vickers microhardness tester, with 25 gf load. Conversion electron Mössbauer spectroscopy (CEMS) was performed at room temperature with a conventional constant-acceleration velocity Mössbauer spectrometer. The samples were inserted into a proportional gas flow counter through which a gas mixture of He with 5% CH_4 was allowed to flow. The CEM spectra were evaluated with the aid of the NORMOS least-squares fitting routine.[23]

Auger electron spectroscopy (AES) depth profiling was performed with a MICROLAB 310F (Fisons Instruments) with a field emission electron source (energy of the primary electrons of 10 keV) and hemispherical sector analyzer. Samples were sputtered with 3 keV Ar ions at current densities of about 1 μA/mm^2. To get smooth crater surfaces and to exclude topography effects, samples were rotated during sputtering. Etch rates of up to 0.5 nm/s were reached. For C, N, and O the KLL-Auger peaks at kinetic energies of 268, 383, and 506 eV were used while for Cr, Fe, and Ni, the LMM-Auger peaks at kinetic energies of 532, 703, and 821 eV were used, respectively. Glow discharge optical spectroscopy (GDOS) depth profiling analysis was performed in a JY-5000RF (Jobin–Yvon) machine.

III. RESULTS AND DISCUSSIONS

The two-cycle plasma nitriding was applied to AISI 304, combining HPN and LPN cycles in the standard gas mixture. The standard gas mixture plasma was used to produce a high temperature (400–450 °C) on the samples and the substrate holder, when running the discharge at high pressure and bias in the -600 to -800 V range. In the case of high-pressure glow discharge, with a mean-free path of about 0.13 cm, the final acceleration of the nitrogen ions that impinge on the surface to be treated is reduced by inelastic collisions and, in the low-pressure cycle, with a mean-free path of about 65 cm, the higher effective acceleration of the nitrogen ions allows deeper penetration of the ions into the sample surface.[24,25] In this case, the plasma was produced by the secondary power supply running at 900 V and 80 mA, while a bias of -700 to -1000 V was applied to the sample holder. The current flowing through the sample holder was lower than 30 mA, in an area of about 100 cm^2.

For a comparison, the x-ray diffraction (XRD) spectrum of the standard AISI 304 is presented in the Fig. 2(a). Apply-

Downloaded 13 May 2013 to 150.163.34.35. This article is copyrighted as indicated in the abstract. Reuse of AIP content is subject to the terms at: http://jap.aip.org/about/rights_and_permissions

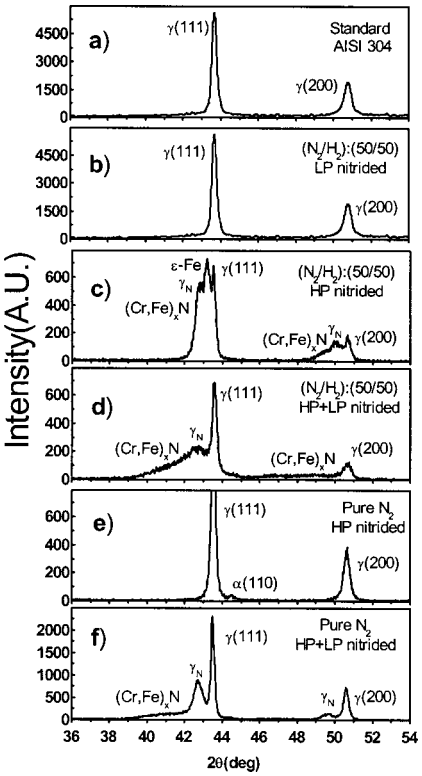

FIG. 2. XRD patterns of treated AISI 304. (a) Reference AISI 304. (b) Treated in the standard gas mixture, applying only LPN, 8×10^{-4} mbar. (c) Treated in standard gas mixture, applying only HPN, 4×10^{-1} mbar. The peaks of the γ_N, the expanded austenite are very intense, aside the presence of iron and chromium nitrides. (d) Treated in the standard gas mixture, alternating cycles of HPN and LPN. Very broad peaks of the γ_N, the expanded austenite and iron and chromium nitrides are present. (e) Treated in pure N_2, applying only HPN. The treatment induced an α-phase layer. (f) Treated in pure N_2, alternating cycles of HPN, and LPN. γ_N, the expanded austenite and iron and chromium nitrides are present.

ing only LPN and the standard gas mixture caused no noticeable modification in the XRD of the samples, as can be seen in the Fig. 2(b). When only the HPN cycle was applied to the samples using the standard gas mixture, the XRD spectrum showed the presence of γ_N, the ϵ phase and mixed nitrides of chromium and iron. The XRD patterns resulting from this treatment can be seen in the Fig. 2(c). The best results so far were attained applying the standard gas mixture and the two-cycles process five times, performing 150 min of nitriding, although the number of cycles could be extended as much as needed. The XRD result of the samples treated by such a process showed very intense γ_N peaks and a large amount of mixed nitrides of chromium and iron. This feature can be seen on the left-hand side of $\gamma(111)$ and other diffraction peaks in Fig. 2(d). When only HPN cycle with pure N_2 was applied, the results of XRD showed the presence of martensite, the α-phase aside the austenite, as presented in Fig. 2(e). Treatment in pure N_2 alternating HPN cycles and LPN cycles produced a large amount of γ_N, and mixed nitrides of chromium and iron, as can be seen in the Fig. 2(f). The measured lattice parameter of some samples is presented in Table I. According to literature values,[5,9,16] Fig. 2 correspond to N contents in excess of 4×10^{18} N/cm^2, in the case of the expanded austenite of the samples in Figs. 2(c)–2(e).

TABLE I. The cubic lattice parameter a (Å) of the nitrided samples.

Phase	Literature[a,b,c]	Encountered
$\gamma(111)$, fcc[d]	3.60	3.60
γ_N, fcc	3.73	3.74
$\alpha(110)$, bcc[e]	2.87	2.88
ϵ, hcp[f]	Not measured	

[a]See Ref. 9.
[b]See Ref. 10.
[c]See Ref. 15.
[d]fcc indicates face centered cubic.
[e]bcc indicates body centered cubic.
[f]hcp indicates hexagonal close packed.

AES profiling performed on the sample treated under the standard gas mixture and the two-cycle process five times, performing 150 min of nitriding, showed that the penetration of the nitrogen into the surface exceeds 700 nm. Even at this distance from the surface, the nitrogen concentration is about 20 at. %, as can be seen in Fig. 3. Also in Fig. 3, it is worth noting the small amounts of carbon and oxygen into the near surface, almost zero. These results can be ascribed to a synergistic effect of several factors, viz.:

(1) The high temperature attained in the HP cycle, that allows for a high diffusion rate of the nitrogen into the surface,
(2) The lower kinetic energy loss possible to the ions at low pressure, allowing for a higher kinetic energy of the nitrogen ions hitting the surface, probably enough to surpass the thin oxide layer, then diffusing inward to the surface,
(3) The presence of hydrogen, removing oxygen and oxides on the surface,
(4) A more effective sputter rate, possible at low pressure.

The AES results of the sample treated under HPN and the standard gas mixture showed that the range of nitrogen is around 650 nm with a maximum of 15 at. % at 90 nm and a great amount of oxygen into the surface, increasing to 56 at. % at 50 nm. This result can be ascribed to lower hydrogen mobility at higher pressures and a lower sputter rate due to the greater collision energy loss of the sputtering ions. Car-

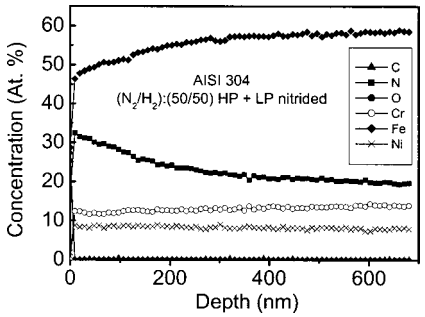

FIG. 3. AES of nitrided AISI 304, in the standard gas mixture. Treatment alternating cycles of HPN and LPN. The nitrogen concentration is more than 20 at. % at 700 nm. Impurities, like oxygen and carbon, are nearly zero even at the surface.

Downloaded 13 May 2013 to 150.163.34.35. This article is copyrighted as indicated in the abstract. Reuse of AIP content is subject to the terms at: http://jap.aip.org/about/rights_and_permissions

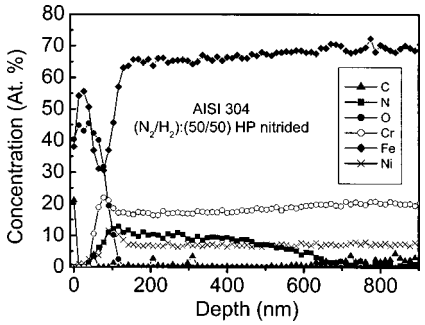

FIG. 4. AES of nitrided AISI 304, in the standard gas mixture, applying only HPN. The nitrogen range is about 650 nm. Carbon impurities are in a very little amount at the surface and at 800 nm, it is ascribed to AES noise. Oxygen impurities range from the surface to around 100 nm, with the peak of 45 at. % at 50 nm.

bon is present in a small quantity near the surface. Oxygen probably is combined as oxides of AISI 304 components, as can be inferred from Fig. 4.

CEM spectra were measured at the ion-treated samples and compared with an untreated reference one. The spectrum of the reference sample is the typical one of nonmagnetic austenitic stainless steel. It consists of a singlet with an isomer shift $\delta = -0.109$ mm/s, in reference to α-Fe, which is well known from literature. This spectrum can be seen in Fig. 5(a).

The CEM spectrum of the sample treated under LPN and the standard gas mixture does not contain magnetic components. It can be decomposed into two singlets, one of the original austenite (67.0%) and a second broad one of expanded austenite (33.0%), Fig. 5(b). The hyperfine parameters of the iron nitrides used for the phase analysis were taken from Schaaf.[26]

The spectrum of the sample treated under HPN and the standard gas mixture can only be understood in connection with the measured concentration profile, Fig. 4. The profile shows a large amount of oxygen in the first 100 nm while the nitrogen profile starts only at about 50 nm and reaches its maximum when the oxygen drops down nearly completely. Although the stainless steel contains about 18 at. % chromium, nothing is found during the first 50 nm. The behavior of the nickel (about 8 at. % in the bulk) is quite similar.

The probe depth for CEMS is about 200 to 300 nm for steel, but the main part of the signal, namely about 65%, comes from the first 50 nm. Contributions of deeper layers are underemphasized in the spectrum. The spectrum consist of a broad single line which can best be decomposed by two singlets: One with the isomer shift of the untreated sample (44.5%), the other one with $\delta = 0.138$ mm/s, (55%). Taking into account the AES results, this singlet can be ascribed to nonstoichiometric iron oxide. The stoichiometric oxides Fe_2O_3 or Fe_4O_3 can be excluded because they would produce a magnetic six-line pattern in the spectrum. Maybe a small amount of ϵ-Fe_2N is hidden within the broad doublet but it can neither be proved nor excluded by Mössbauer spectroscopy. However, this result can be confirmed by the XRD spectrum of the Fig. 2(c), where we can see one peak of the ϵ-iron phase.

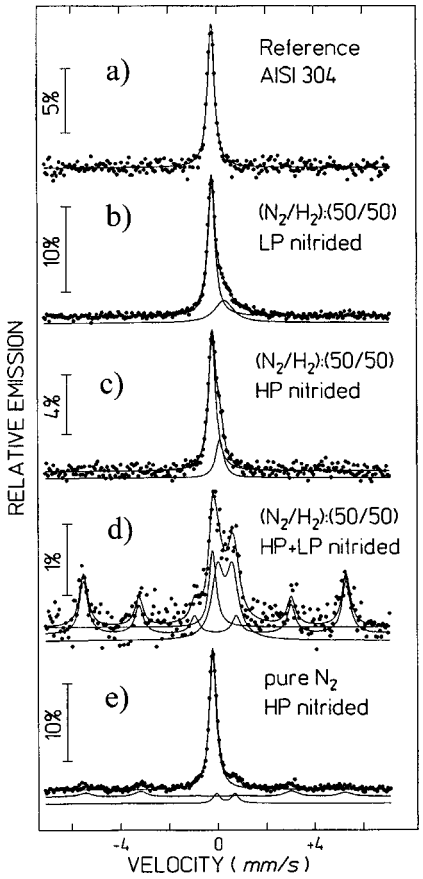

FIG. 5. CEMS patterns of the nitrided AISI 304 samples. (a) Reference AISI 304 sample. (b) Samples treated in the standard gas mixture applying only LPN. (c) Samples treated in the standard gas mixture, applying only HPN. (d) Samples treated in the standard gas mixture, alternating cycles of HPN, and LPN. (e) Samples treated in pure N_2 and HPN.

The existence of the singlet of the stainless steel shows that a large part of the iron atoms is not influenced by the ion treatment and is still in the same environment as before the treatment, as can be seen in the Fig. 5(c).

The AES depth profiles and the CEM spectrum of the sample treated under HPN plus LPN and the standard gas mixture are very different from those samples treated under other nitriding sequences. While the depth profile shows a continuous decrease of the nitrogen from the surface to the bulk starting with about 33 at. %, Fig. 3, the CEM spectrum consists of both magnetic and non-magnetic components. A small fraction of the singlet of stainless steel (14.5%) is still observed. But main components are now a magnetic six-line-pattern (44.0%) with hyperfine parameters close to those of α-Fe (α-Fe: $\delta = 0.000$ mm/s, inner magnetic field $B_{HI} = 33.0$ T, measured here: $\delta = 0.005$ mm/s, $B_{HI} = 33.5$ T) and a broad doublet (41.5%) with $\delta = 0.300$ mm/s and a quadrupole splitting $\Delta = 0.601$ mm/s. The latter could be ascribed to ϵ-Fe_2N influenced due to the chromium, while the sextet denotes martensitic fractions, Fig. 5(d).

As the probing depth of CEMS is about 300 nm, information beyond this range is inferred from other techniques. The AES technique showed about 20 at. % of nitrogen even at depths as far as 700 nm. Preliminary GDOS depth profiling showed a nitrogen range exceeding 2 μm, in agreement

Downloaded 13 May 2013 to 150.163.34.35. This article is copyrighted as indicated in the abstract. Reuse of AIP content is subject to the terms at: http://jap.aip.org/about/rights_and_permissions

TABLE II. Vickers hardness with 25 gf load resulting from different nitriding processes, and 150 min of total treatment time. AISI 304 reference hardness: 200 HV.

Treatment	$HV_{0.025}$ (Hardness enhancement)
(a) Combined plasma nitriding, (N_2/H_2):(50/50), 15 min HPN,[a] 450 °C, alternating with 15 min, LPN,[b] 330 °C, five cycles of each	542 (2.7×)
(b) Combined plasma nitriding, similar to treatment (a), but with pure N_2, 150 min	327 (1.6×)
(c) HPN, (N_2/H_2):(50/50), 450 °C, 150 min	356 (1.8×)
(d) HPN, pure N_2, 450 °C, 150 min	348 (1.7×)
(e) LPN, (N_2/H_2):(50/50), 270 °C, 150 min	220 (1.0×)

[a]HPN=High-pressure nitriding, 4×10^{-1} mbar.
[b]LPN=Low-pressure nitriding, 8×10^{-4} mbar.

with the XRD, whose probing depth is about 2.5 μm, as shown by the presence of γ_N, in Fig. 2(d). This diffusion zone is of much importance to the enhanced tribological properties of the treated AISI 304 surface.

The sample treated under HPN and pure N_2 looks very inhomogeneous and its CEM spectrum was taken including all the treated regions of the sample. The evaluation of the CEM spectrum gives 70.8% austenite, 19.5% martensite ($B_{HI}=33.1$ T, which is very close to α-Fe, again), and 9.7% expanded austenite, Fig. 5(e). This result agrees well with the XRD spectrum of Fig. 2(e), where we can see the peak of the martensite.

Vickers hardness measurements of the samples showed that applying the two-cycle nitriding and the standard gas mixture, produced a hard layer, with a hardness about 540. When pure N_2 or the standard gas mixture was applied to the samples in manners other than that combining the standard gas mixture and the two-cycle nitriding, the Vickers hardness presented values between 1.0 and 1.8 times the standard AISI 304 hardness of about 200 HV, as shown in Table II.

IV. CONCLUSION

Hybrid plasma treatment combining high- and low-pressure ion nitriding was tested. The two-cycle nitriding process, combining high-pressure and high-temperature stage followed by lower-pressure nitriding with a mixture of nitrogen and hydrogen showed good results, when applied to the AISI 304.

The best results were obtained from the sequential nitriding, under the (N_2/H_2):(50/50) gas mixture, in two steps: The first ion nitriding at 4×10^{-4} mbar pressure, when the samples reach a high temperature, near 450 °C, followed by a low-pressure glow ion nitriding, at 8×10^{-4} mbar. In this cycle, the initial temperature, around 450 °C goes down to around 300 °C, when the treatment is stopped. This low-pressure cycle takes advantage of the high temperature attained in the first cycle and the higher mean-free path, possible at lower pressures, ensuring higher impinging energies of the nitrogen ions on the sample surface. The thick modified layer, thus created, with surface hardness of 2.7 times the standard nontreated surface value, presented mainly the presence of γ_N, the expanded austenite, and mixed chromium and iron nitrides. Oxygen and carbon as impurities are present only in small quantities at the very near surface. Other combinations of gas mixture and cycles did not present results as good as well, and the presence of the contaminants as oxygen and carbon are in greater amounts, as confirmed by the AES of the samples treated under the mixture of (N_2/H_2):(50/50) and only applying the high-pressure cycle. The proper identification of the phases and compounds by XRD was greatly facilitated by analyzing CEMS and AES results, which clarified some doubts about the presence of iron oxides and the presence of the layer of martensite, as presented by the samples treated under pure N_2, and applying only the high-pressure cycle.

ACKNOWLEDGMENTS

This work was partially funded by FAPESP. One of the authors (G. F. G.) also acknowledges FAPESP for a postdoctoral fellowship.

[1] *Handbook of Plasma Immersion Ion Implantation and Deposition*, edited by J. André Anders, 1st ed. (Wiley, Toronto, 2000).
[2] E. Menthe and K. T. Rie, Surf. Coat. Technol. **112**, 217 (1999).
[3] J. M. O'Brien, *Plasma (Ion) Nitriding, ASM Handbook* (ASM International Handbook Committee, Metals Park, OH, 1994), Vol. 4.
[4] B. Larisch, U. Brusky, and H.-J. Spies, Surf. Coat. Technol. **116**, 205 (1999).
[5] R. Wei, J. J. Vajo, J. N. Matossian *et al.*, Surf. Coat. Technol. **83**, 235 (1996).
[6] M. Berg, C. V. Budtz-Jørgensen, H. Reitz *et al.*, Surf. Coat. Technol. **124**, 25 (2000).
[7] S. Mändl, R. Günzel, E. Richter, and W. Möller, Surf. Coat. Technol. **100**, 372 (1998).
[8] R. Günzel, M. Betzel, I. Alphonsa *et al.*, Surf. Coat. Technol. **112**, 307 (1999).
[9] H. Pelletier *et al.*, Nucl. Instrum. Methods Phys. Res. B **148**, 824 (1999).
[10] M. Guemmaz, A. Mosser, J.-J. Grob, and R. Stuck, Surf. Coat. Technol. **100**, 353 (1998).
[11] M. K. Lei and Z. L. Zhang, Surf. Coat. Technol. **91**, 25 (1997).
[12] G. A. Collins, R. Hutchings, K.-T. Short, and J. Tendys, Surf. Coat. Technol. **103**, 212 (1998).
[13] C. Blawert, Y. Jiráskova, B. L. Mordike, and O. Schneeweiss, Surf. Coat. Technol. **116**, 189 (1999).
[14] R. Grün and H.-J. Günther, Mater. Sci. Eng., A **140**, 435 (1991).
[15] H. Michel *et al.*, Surf. Coat. Technol. **72**, 103 (1995).
[16] M. P. Fewell *et al.*, Surf. Coat. Technol. **131**, 300 (2000).
[17] M. Ueda, G. F. Gomes, E. Abramof, and H. Reuther, Nucl. Instrum. Methods Phys. Res. B **206**, 749 (2003).
[18] M. Ueda, L. A. Berni, G. F. Gomes, A. F. Beloto, E. Abramof, and H. Reuther, J. Appl. Phys. **86**, 4821 (1999).
[19] C. V. Budtz-Jørgensen, Ph.D. thesis, Aarhus University, 2001.
[20] Y. Hirohata, N. Tsuchiya, and T. Hino, Appl. Surf. Sci. **169**, 612 (2001).
[21] S. Kumar *et al.*, Surf. Coat. Technol. **123**, 29 (2000).
[22] M. Kopcewicz, J. Jagielski, G. Gawlik, and A. Turos, Nucl. Instrum. Methods Phys. Res. B **68**, 417 (1992).
[23] R. A. Brand, University of Duisburg, Germany.
[24] S. Leigh *et al.*, Surf. Coat. Technol. **85**, 37 (1996).
[25] B. Chapman, *Glow Discharge Processes: Sputtering and Plasma Etching* (Wiley, New York, 1980).
[26] P. Schaaf, Hyperfine Interact. **111**, 113 (1998).

Downloaded 13 May 2013 to 150.163.34.35. This article is copyrighted as indicated in the abstract. Reuse of AIP content is subject to the terms at: http://jap.aip.org/about/rights_and_permissions